

Determining the Relative Reactivity of Sulfate, Bisulfate, and Organosulfates with Epoxides on Secondary Organic Aerosol

Erika Aoki, Jon N. Sarrimanolis, Sophie A. Lyon, and Matthew J. Elrod*

Cite This: *ACS Earth Space Chem.* 2020, 4, 1793–1801

Read Online

ACCESS |



Metrics & More



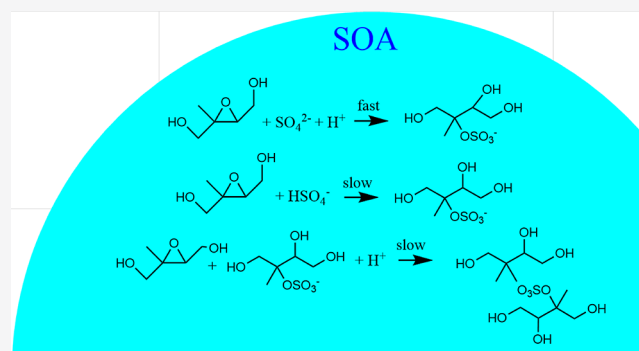
Article Recommendations



Supporting Information

ABSTRACT: Extensive laboratory and field studies have identified nucleophilic addition reactions of isoprene epoxydiols (IEPOX) as key pathways for the formation of isoprene-derived secondary organic aerosol (SOA). Organosulfates are important reaction products of these processes, but it is unclear whether sulfate and/or bisulfate nucleophiles are responsible for their formation and whether the organosulfates themselves can serve as nucleophiles in oligomer-forming reactions. The relative reactivities (nucleophilic strengths relative to water) of sulfate, bisulfate, and methyl sulfate anion were measured through a series of model epoxide–nucleophile experiments using nuclear magnetic resonance (NMR) spectroscopy. These experiments also helped establish a rigorous understanding of the effects of differing carbon substitution and functional groups of epoxides on the modulation of the effective nucleophilicities of sulfate, bisulfate, and methyl sulfate anions. It was determined that the nucleophilicities of bisulfate and methyl sulfate anions were about 100 and 50 times, respectively, weaker than sulfate toward most of the epoxides studied, which was rationalized by computational estimates of their thermodynamic basicities. Therefore, for most SOA acidity situations, sulfate–epoxide reactions are expected to be the main source of organosulfate aerosol constituents. Because sulfate–epoxide reactions stoichiometrically consume acid, these reactions also have the capability of raising the pH of SOA, thus slowing down all acid-catalyzed chemical processes. No evidence for the reaction of the methyl sulfate anion was observed with the abundant atmospherically relevant epoxide, *trans*- β -IEPOX, thus suggesting that oligomerization reactions via epoxide–organosulfate reactions may not be able to compete with stronger (such as sulfate) or more abundant (such as water) nucleophiles on actual SOA.

KEYWORDS: atmosphere, air pollution, isoprene, thermodynamics, basicity, kinetics, nucleophilicity, nuclear magnetic resonance



INTRODUCTION

Secondary organic aerosol (SOA),¹ which makes up a significant portion of the atmosphere's particulate matter, has been implicated in human respiratory and cardiovascular diseases,^{2,3} visibility loss,⁴ and climate modification.⁵ Isoprene, the dominant nonmethane hydrocarbon in the atmosphere, is thought to contribute significantly to SOA formation and growth^{6,7} via its oxidation intermediates, isoprene epoxydiols (IEPOX).⁸ Laboratory and field studies have showed that IEPOX can lead to the formation of the known SOA components 2-methyltetrol and its sulfate derivatives through acid-catalyzed, condensed-phase, nucleophilic addition reactions of IEPOX.^{8–17} However, it remains unclear whether sulfate (SO_4^{2-}) and/or bisulfate (HSO_4^-) are the key nucleophiles in the formation of organosulfate products on SOA. In addition to the likely differing reactivities (or more specifically, nucleophilicities) of sulfate and bisulfate, Figure 1 also explicitly shows that while the role of acids in bisulfate nucleophilic reactions is strictly catalytic, acids also play a stoichiometric role in sulfate nucleophilic reactions. This is an

important distinction because the potential consumption of acids by IEPOX reactions would then serve to slow down all acid-catalyzed SOA reactions. Indeed, it has been shown that under high IEPOX conditions, significant consumption of inorganic sulfate can occur,¹⁸ which suggests that IEPOX reactions may also be capable of changing SOA pH if sulfate nucleophilic reactions are indeed the dominant reaction process.

In addition, recent work has suggested that previous attempts to quantify the individual species derived from IEPOX reactions may have underestimated the presence of oligomeric products.^{19–22} Such oligomers may have profound effects on aerosol properties, including aerosol particle

Received: July 6, 2020

Revised: September 1, 2020

Accepted: September 10, 2020

Published: September 10, 2020



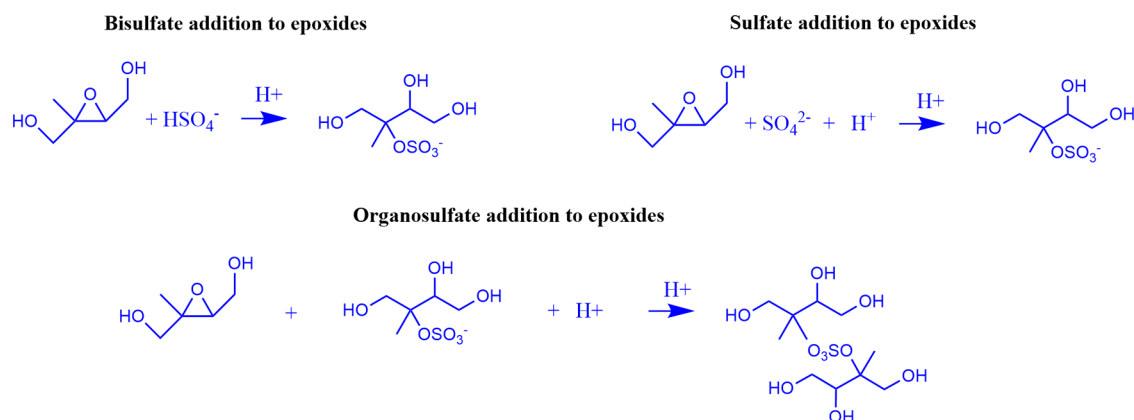


Figure 1. Potential IEPOX-derived organosulfate-forming mechanisms.

viscosity and the rates of diffusion and evaporative processes,²³ and therefore have important implications for regional and global aerosol models.^{19,24,25} However, the mechanisms by which such oligomers may form remain unclear.²⁶ Since the IEPOX-derived organosulfates form via nucleophilic addition reactions of SO_4^{2-} and/or HSO_4^- , and the organosulfate derivatives themselves are of the form RSO_3^- at ambient SOA pH levels, it is possible that oligomers could form via the nucleophilic addition of the organosulfate derivatives to IEPOX via the mechanism shown in Figure 1.

In the present study, we use model bulk sulfate/bisulfate aqueous solutions and the Extended Aerosol Inorganics Model (E-AIM)²⁷ to parameterize the nucleophilicity of sulfate and bisulfate relative to water for a number of model epoxides using nuclear magnetic resonance (NMR) as the primary analytical technique. The bulk solution method allows for careful control over reactant and catalyst species, as well as their concentrations, and the NMR method can be used to determine isomer-specific structures and relative concentrations for product species.^{26,28} We also systematically investigate the carbon substitution and functional group dependence of various epoxides in their nucleophilic reactions with sulfate and that of a model organosulfate, methyl sulfate anion ($\text{CH}_3\text{OSO}_3^-$), in order to assess the likelihood of oligomer-forming nucleophilic addition of organosulfates to epoxide reactions on SOA.

METHODS AND MATERIALS

Chemicals. The following commercially available chemicals were used from MilliporeSigma ((\pm)-propylene oxide, 99%; (*R*)-(+)-glycidol, 97%; epifluorohydrin, 98%; (\pm)-epichlorohydrin, 99%; epibromohydrin, 98%; *cis*-2,3 epoxybutane, 97%; 1,2-epoxybutane, 99%; 2-methyl-1,2-epoxypropane, 97%; 2,3-dimethyl-2,3-epoxybutane, 99%; sodium sulfate, 99%; sodium bisulfate, 99%; methyl sulfate sodium salt, sulfuric acid- d_2 solution, 96–98 wt % in D_2O , 99.5 atom % D; and perchloric acid- d solution, 68 wt % in D_2O , 99 atom % D) and Cambridge Isotope Laboratories, Inc. (deuterium oxide, 99.5% and sodium 2,2-dimethyl-2-silapentane-5-sulfonate (DSS), 97%). A sample containing *cis*-2,3-epoxy-1,4-butanediol and a sample containing *trans*- β -IEPOX were each prepared and characterized according to separate procedures previously reported by our lab.^{9,29}

Nucleophilic Strength Experiments. The molal activity-based sulfate and bisulfate nucleophilic strengths of 1,2-epoxybutane, *cis*-2,3-epoxybutane, and 2-methyl-1,2-epoxybu-

tane were determined by reacting them in two solution sets of either varying sulfate concentrations (solution set 1) or varying bisulfate concentrations (solution set 2) as indicated in Table S1. For solution set 1, differing amounts of sodium sulfate were added to 0.1 M $\text{D}_2\text{SO}_4/\text{D}_2\text{O}$ solutions. For solution set 2, differing amounts of sodium bisulfate were added to D_2O . In order to determine their mole fraction-based SO_4^{2-} and $\text{CH}_3\text{OSO}_3^-$ nucleophilic strengths, all epoxides were reacted in either 0.1 M $\text{D}_2\text{SO}_4/0.9$ M $\text{Na}_2\text{SO}_4/\text{D}_2\text{O}$ or 0.1 M $\text{DClO}_4/5.0$ M $\text{CH}_3\text{OSO}_3\text{Na}/\text{D}_2\text{O}$ solutions, respectively. All reactions were run in bulk solutions with total volumes of 750 μL (the amount required for NMR analysis) with either 10 or 50 μL of epoxide added. Using their acid-catalyzed ring opening rate constants, the pseudo-first-order lifetime of each epoxide was calculated and the solutions were allowed to react for at least three lifetimes to ensure that the epoxide reactant was completely consumed before the NMR analysis was performed.

Acid-Catalyzed Epoxide Ring Opening Kinetics Experiments. The acid-catalyzed ring opening rate constants for many of the epoxides in the present study had been previously studied. However, for the epoxides for which no appropriate literature kinetics data could be found for their acid-catalyzed ring opening rates in dilute aqueous solutions at room temperature (propylene oxide, glycidol, epifluorohydrin, epichlorohydrin, epibromohydrin, and *cis*-2,3-epoxybutane), their second-order rate constants were measured according to the following procedure. In order to achieve a pseudo-first-order lifetime of about 1 h (convenient for NMR monitoring of the kinetics), various $\text{DClO}_4/\text{D}_2\text{O}$ solutions were tested to find an appropriate concentration for the kinetics measurement. The actual kinetics experiment was carried out by adding 10 μL of the epoxide to 750 μL of the appropriate $\text{DClO}_4/\text{D}_2\text{O}$ solution, stirring for 1 min in a 20 mL vial, and immediately transferring the solution to an NMR tube for kinetics monitoring.

NMR Methods. NMR spectra were recorded using a Bruker 400 MHz instrument using built-in pulse sequences, except in cases where an increased number of scans was necessary to enhance the signal-to-noise ratio. ^1H spectra were calibrated to the HDO peak at 4.79 ppm, and most of the ^{13}C spectra were calibrated to the DSS methyl peak at 0.00 ppm (in some cases, secondary calibration was used to achieve a DSS-referenced chemical shift, as indicated in the NMR assignments listed in the Supporting Information). The relative concentrations of the various species were determined by integration of one or more unique peaks in the ^1H or ^{13}C

spectra. Because the ^{13}C nuclei are not fully relaxed for the 1 s relaxation time used in the NMR experiments, care was taken to use similarly substituted nuclei for the relative integration process, and several different sets of integration ratios for differently substituted nuclei were averaged to improve the precision of the calculated relative concentrations. The overall precision of the relative concentration ratios was estimated to be better than 10%. The pseudo-first-order rate constants were determined by linear regression and converted to second-order rate constants by dividing the pseudo-first-order rate constants by the formal concentrations of DClO_4 .

Computations. The thermodynamic basicity (the enthalpy of reaction for the reaction of H_3O^+ with the base to produce the protonated base and H_2O) was computed for SO_4^{2-} , HSO_4^- , and $\text{CH}_3\text{OSO}_3^-$ according to the following procedure. Geometries (determined at the B3LYP/6-31G(d,p) level) and energies of the relevant species were calculated using a modified version of the G2MS compound method (MG2MS),³⁰ variation of the G2 theory.³¹ The Polarizable Continuum Model (PCM) method³² was used to account for the effects of water solvation on the reactant and product properties. All calculations were carried out with the Gaussian 03 and 09 computational suites.³³ Each stationary point was confirmed as a potential energy minimum by inspection of the calculated frequencies. The overall energy expression for the MG2MS scheme is defined in eq 1:

$$E_{\text{elec}}(0\text{ K}) = E_{\text{CCSD(T)/6-31G(d)}} + E_{\text{MP2/6-311+G(2df,2p)}} - E_{\text{MP2/6-31G(d)}} + \text{HLC} \quad (1)$$

where HLC is an empirically defined correction term with $\text{HLC} = An_\alpha + Bn_\beta$, where n_α and n_β are the number of α and β electrons, respectively, and the constants A and B are 6.06 and 0.19 mH, respectively (all species investigated were closed shell; therefore $n_\alpha = n_\beta$). The enthalpy is calculated from eq 2:

$$H(298\text{ K}) = E_{\text{elec}}(0\text{ K}) + E_{\text{zpe}} + E_{\text{thermal}} \quad (2)$$

where E_{zpe} is the zero-point energy and E_{thermal} includes the corrections necessary to adjust the internal energy to 298 K and convert to enthalpy. Our previous MG2MS results for atmospherically relevant systems (including radicals and ions) indicate that the MG2MS-calculated enthalpies of a reaction are typically accurate to within 10 kJ mol⁻¹ for systems similar to those under study here.³⁴

RESULTS AND DISCUSSION

NMR Assignments. As an example of the typical NMR spectra collected for the series of epoxide reaction systems, the ^{13}C NMR spectrum and assignments for all species involved in the glycidol/0.1 M D_2SO_4 /0.9 M $\text{Na}_2\text{SO}_4/\text{D}_2\text{O}$ reaction system are shown in Figure 2. The epoxide reactants were easily distinguishable in the ^1H NMR spectra, and kinetics measurements were made using ^1H peak integrations. On the other hand, assignments and quantifications of products were primarily made using ^{13}C NMR methods as the ^1H NMR spectra were frequently uninterpretable as a result of an extensive chemical shift overlap between the various nucleophilic addition products. Full ^{13}C NMR spectral assignments (and some ^1H NMR assignments) are given for all species in the Supporting Information.

$\text{HSO}_4^-/\text{SO}_4^{2-}$ Molal Activity-Based Nucleophilic Strengths. In order to allow the detection of relatively

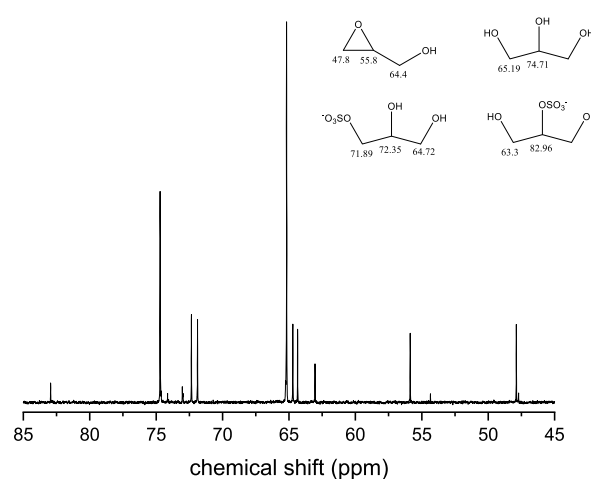


Figure 2. ^{13}C NMR spectrum of the glycidol/0.1 M D_2SO_4 /0.9 M $\text{Na}_2\text{SO}_4/\text{D}_2\text{O}$ reaction system.

small yields of certain nucleophilic addition products, high concentrations of nucleophiles were used in most experiments, leading to potentially important nonideal solution effects. In the case of sulfuric acid/sodium sulfate/water systems, the Extended AIM Aerosol Thermodynamics Model²⁷ was used to calculate the molal-based activities ($a = \gamma \times m$) of the various inorganic species, which are given in Table S1. The nucleophilic strength (NS_1) of a nucleophile (nucleophile 1) relative to the nucleophilic strength (NS_2) of a different, competing nucleophile (nucleophile 2) also present in a given system can be determined from the initial nucleophile activities (a) and final nucleophilic addition product mole fraction (Y) via eq 1:

$$\frac{\text{NS}_1}{\text{NS}_2} = \frac{(Y_1/a_1)}{(Y_2/a_2)} \quad (3)$$

By defining all nucleophilic strengths relative to the hydrolysis reaction (water as nucleophile 2 and $\text{NS}_{\text{water}} = 1$), eq 3 can be expressed as:

$$\frac{Y_{\text{nuc}}}{Y_{\text{water}}} a_{\text{water}} = \text{NS}_{\text{nuc}} a_{\text{nuc}} \quad (4)$$

Therefore, a plot of $(Y_{\text{nuc}}/Y_{\text{water}}) a_{\text{water}}$ versus a_{nuc} will yield a line with a slope equal to NS_{nuc} . In the present case where both the sulfate and bisulfate nucleophiles can lead to the same nucleophilic addition product, eq 4 can be defined for the situation in which both nucleophiles are active:

$$\frac{Y_{\text{nuc}}}{Y_{\text{water}}} a_{\text{water}} = \text{NS}_{\text{sulfate}} a_{\text{sulfate}} + \text{NS}_{\text{bisulfate}} a_{\text{bisulfate}} \quad (5)$$

Therefore, via eq 5, multiple linear regression methods can be used to determine the nucleophilic strengths, $\text{NS}_{\text{sulfate}}$ and $\text{NS}_{\text{bisulfate}}$. Since solution set 1 was designed to vary a_{sulfate} while holding $a_{\text{bisulfate}}$ largely constant, and solution set 2 was designed to vary $a_{\text{bisulfate}}$ while holding a_{sulfate} largely constant, in principle, the data can also be analyzed via single linear regression methods and eq 4. Table 1 lists the results of both the single (solution set 1 data) and multiple linear regression approaches (solution set 2 data and all data) for the nucleophilic reactions of 1,2-epoxybutane for solution set 1; however, it was found that because sulfate is such a strong nucleophile relative to bisulfate, solution set 2 could not be

Table 1. Molal Activity-Based Nucleophilic Strength (and 1 σ Uncertainties) Linear Regression Results for 1,2-Epoxybutane

	primary sulfate product		secondary sulfate product	
	NS _{sulfate}	NS _{bisulfate}	NS _{sulfate}	NS _{bisulfate}
solution set 1 data	233.8 \pm 7.8		213.3 \pm 9.0	
solution set 2 data	160 \pm 14	2.28 \pm 0.16	156.9 \pm 7.8	0.755 \pm 0.089
all data	211.4 \pm 9.3	1.95 \pm 0.19	198.2 \pm 7.7	0.49 \pm 0.15

adequately analyzed via single linear regression methods (because the small variations in a_{sulfate} were enough to invalidate the single regression analysis using only changes in $a_{\text{bisulfate}}$). Table 2 summarizes the relevant regression analyses for the nucleophilic strengths of the reactions of 1,2-epoxybutane.

The multiple linear regression results for the entire data set are largely consistent with the single and multiple linear regression results for solution sets 1 and 2. As will be seen for the other two epoxides extensively studied and discussed below, only 1,2-epoxybutane has some NS values that do not fall within the 95% confidence interval of each other for the three data sets. For some solutions for 1,2-epoxybutane only, there was some NMR signal overlap, which probably caused larger errors in the determination of the $Y_{\text{nuc}}/Y_{\text{water}}$ ratios used in the regression analyses. The use of activities calculated from the E-AIM model, rather than the formal concentrations of sulfate and bisulfate, was critical for the success of the approach as the attempted use of formal concentrations in eq 3 leads to physically unreasonable negative nucleophilic strength values for bisulfate. Because some of the solutions are strongly nonideal, this was not an unexpected result.

The 1,2-epoxybutane system is particularly interesting as there are two distinguishable nucleophilic addition products. The present results show that the nucleophilic strengths for sulfate for both reaction sites are statistically identical, while the nucleophilic strengths for bisulfate are significantly less for a reaction at the secondary position. This suggests that the mechanism for the secondary attack by bisulfate is more affected by steric hindrance than it is for sulfate. Since bisulfate and sulfate are virtually of the same size, this result implies that mechanisms for sulfate and bisulfate attack are different, with the bisulfate reaction occurring via a more pure concerted A-2 mechanism (similar to the nucleophilic substitution mechanism, S_N2).³⁵ The results also indicate that the nucleophilic strength of bisulfate is more than 100 times weaker than that of sulfate and similar to that of water (slightly more nucleophilic than water for attack at the primary position and slightly less nucleophilic than water for attack at the secondary position). Because nucleophilicity is most closely correlated with the property of basicity,³⁶ this result may be qualitatively rationalized by the greater basicity of sulfate as compared to bisulfate and water.

Similar analyses are reported for *cis*-2,3-epoxybutane and 2-methyl-1,2-epoxybutane in Tables 2 and 3, respectively.

For *cis*-2,3-epoxybutane, the sulfate nucleophilic strength is statistically indistinguishable from that for 1,2-epoxybutane, while the value for the bisulfate nucleophilic strength is midway between the primary and secondary attack sites for 1,2-epoxybutane. For 2-methyl-1,2-epoxybutane, both the sulfate and bisulfate nucleophilic strengths were found to be

Table 2. Molal Activity-Based Nucleophilic Strength (and 1 σ Uncertainties) Linear Regression Results for *cis*-2,3-Epoxybutane

	secondary sulfate product	
	NS _{sulfate}	NS _{bisulfate}
solution set 1 data	210 \pm 16	
solution set 2 data	161 \pm 11	1.48 \pm 0.10
all data	197 \pm 12	1.27 \pm 0.19

Table 3. Molal Activity-Based Nucleophilic Strength (and 1 σ Uncertainties) Linear Regression Results for 2-Methyl-1,2-Epoxybutane

	tertiary sulfate product	
	NS _{sulfate}	NS _{bisulfate}
solution set 1 data	248 \pm 15	
solution set 2 data	294 \pm 42	2.83 \pm 0.37
all data	250 \pm 18	3.07 \pm 0.28

somewhat larger. For bisulfate, this is an interesting result because the tertiary attack site is more sterically crowded than the primary and secondary sites in 1,2-epoxybutane and *cis*-2,3-epoxybutane, again suggesting that the subtle details of the mechanism must be considered in addition to the simple steric arguments.

Computed Thermodynamic Basicity Values for Sulfate, Bisulfate, and CH₃OSO₃[−]. In order to understand the main causes of the substantially lower nucleophilicity for bisulfate as compared to sulfate and to predict the nucleophilicity of the methyl sulfate anion, the thermodynamic basicity values obtained from the MG2MS method were compared. The values of $\Delta H_{\text{basicity}}$ were determined to be −42.2, −21.8, and −20.7 kcal mol^{−1} for sulfate, bisulfate, and methyl sulfate anions, respectively. These values are correlated almost perfectly with the differing negative charge on various species and suggest that the presence of the alkyl group in the methyl sulfate anion does little to affect the basicity of that species as compared to bisulfate. Therefore, to the extent that basicity is a measure of nucleophilicity, the nucleophilic strength of the methyl sulfate anion is expected to be similar to that of bisulfate. This is also likely true for the larger organosulfates present on SOA.

SO₄^{2−}/CH₃OSO₃[−] Mole Fraction-Based Nucleophilic Strengths. Because the E-AIM model does not have the capability to calculate activities for methyl sulfate anion-containing solutions, a more approximate approach (i.e., one that does not take into account solution nonideality) was used to estimate the nucleophilic strengths of this species. In this case, a mole fraction-based nucleophilic strength was determined in which the activities in eq 1 are replaced by the mole fraction (X) of the nucleophiles:

$$\frac{NS_1}{NS_2} = \frac{(Y_1/X_1)}{(Y_2/X_2)} \quad (6)$$

Again, defining water as nucleophile 2 and $NS_{\text{water}} = 1$ for the reference hydrolysis reaction, the nucleophilic strength of the competing nucleophile can be determined:

$$NS_{\text{nuc}} = \frac{(Y_{\text{nuc}}/X_{\text{nuc}})}{(Y_{\text{water}}/X_{\text{water}})} \quad (7)$$

Table 4. Acid-Catalyzed Second-Order Ring Opening Epoxide Rate Constants and Mole Fraction-Based Sulfate and Methyl Sulfate Nucleophilic Strength values^a

system	k_{H^+} ($\text{M}^{-1} \text{s}^{-1}$)	LS $\text{NS}_{\text{sulfate}}$	MS $\text{NS}_{\text{sulfate}}$	LS $\text{NS}_{\text{CH}_3\text{OSO}_3^-}$	MS $\text{NS}_{\text{CH}_3\text{OSO}_3^-}$
propylene oxide	0.0977	7.4	10.3	0.2	0.2
glycidol	0.011	21.0	4.5	0.4	0.2
epifluorohydrin	0.0019	30.6	2.3	0.6	not observed
epichlorohydrin	0.00121	32.5	0.8	0.5	not observed
epibromohydrin	0.00080	31.1	1.3	0.6	not observed
<i>trans</i> -2,3-epoxybutane	0.20 ³⁷	not applicable	6.9 ³⁷	not measured	not measured
<i>cis</i> -2,3-epoxybutane	0.0885	not applicable	9.0	not applicable	not observed
<i>cis</i> -2,3-epoxy-1,4-butanediol	0.0014 ⁹ , 0.0013 ³⁸	not applicable	24.3, 21 ³⁸	not applicable	1.2
1,2-epoxybutane	0.074 ³⁷	8.0 ³⁷	8.0 ³⁷	0.1	not observed
2-methyl-1,2-epoxypropane	8.7 ³⁷	not observed	9.5 ³⁷	not observed	not observed
2,3-dimethyl-2,3-epoxybutane	15 ⁹	not applicable	3.8 ³⁷	not applicable	not observed
<i>trans</i> - β -IEPOX	0.036 ⁹	not observed	14.0 ¹²	not observed	not observed

^aThe chemical structures for each of the reactant systems are given in the Supporting Information.

Since it is useful to compare the nucleophilic strength of the methyl sulfate anion to sulfate in consideration of the potential competition between sulfate and organosulfates in SOA reactions of epoxides, this approximate method was also applied to sulfate-containing systems even though these experiments could potentially be analyzed via the more rigorous activity-based method described above. Table 4 summarizes the results of this analysis for various epoxide systems, with columns labeled LS for the least-substituted nucleophilic attack site and MS for the most-substituted nucleophilic attack site. For cases in which only one attack site is possible, the results are listed in the MS column and the LS column has a “not applicable” entry. In some cases, a potential isomer was not detected and those cases are indicated with a “not observed” entry. Previous experiments were used to calculate nucleophilic strengths for the reaction with sulfate in several cases, while all methyl sulfate anion results are based on the present work. Previous experiments with *trans*-2,3-epoxybutane were analyzed to calculate nucleophilic strengths for sulfate attack.³⁷ However, this compound is no longer commercially available; therefore, methyl sulfate anion experiments were not performed and this is reflected by “not measured” entries shown in Table 4.

Since the nucleophilic strengths for sulfate reaction with 1,2-epoxybutane, *cis*-2,3-epoxybutane, and 2-methyl-1,2-epoxypropane were determined using both the molal activity-based and mole fraction-based methods, an approximate conversion factor between the two methods can be determined from the molal activity-based values in listed in Tables 1–3 and the mole fraction-based values listed in Table 4.

$$\text{NS}^{\text{molal activity-based}} \approx 20 \times \text{NS}^{\text{mole fraction-based}} \quad (8)$$

As had been reported in previous works, when tertiary attack sites are available, no sulfate reaction at the lesser substituted site is observed.^{12,37,39} However, for every other carbon substitution situation among the various epoxides studied in the present work, all possible sulfate attack reaction products were observed. On the other hand, because of the substantially lower nucleophilic strength of the methyl sulfate anion, many potential nucleophilic attack products were not observed for that reactant. In general, the computational expectation that the nucleophilic strength of the methyl sulfate anion is similar to the weakly nucleophilic bisulfate is borne by the $\text{NS}_{\text{sulfate}}/\text{NS}_{\text{CH}_3\text{OSO}_3^-}$ ratios (~ 50) listed in Table 4 that are similar to the $\text{NS}_{\text{sulfate}}/\text{NS}_{\text{bisulfate}}$ ratios (~ 100) listed in Tables 1–3.

There are a number of interesting structure-reactivity trends apparent in the data listed in Table 4. The influence of functional groups is most readily ascertained by comparing propylene oxide and its various functionalized derivatives. The addition of a hydroxyl group to propylene oxide increases the nucleophilic strength of glycidol at the less substituted site by a factor of three while reducing the nucleophilic strength at the more substituted site by a factor of two as compared to propylene oxide itself. The former effect is probably explained by the electron-withdrawing nature of the functional group, which serves to make the carbon atom more electropositive, while the latter effect is likely rationalized by the steric hindrance introduced by the replacement of the hydrogen atom by a hydroxyl group. The halohydrin series results are also consistent with this explanation. In any case, these findings, in combination with the comparison of the nucleophilic strengths for *cis*-2,3-epoxy-1,4-butanediol with *cis*-2,3-epoxybutane, suggest that neighboring hydroxyl groups serve to boost the overall effective nucleophilic strength of both sulfate and methyl sulfate anions compared to water.

However, most importantly, for assessing the potential atmospheric relevance of organosulfate reactions with atmospherically relevant epoxides, no products resulting from the reaction of the methyl sulfate anion were observed for any of the tertiary substituted epoxides investigated, including *trans*- β -IEPOX, the most atmospherically abundant IEPOX species.⁴⁰ Based on the detection limit determined from systems in which methyl sulfate anion addition products were observed (generally these products could be measured at 0.5–1.0% of the concentration of the sulfate anion addition products), an upper limit for the nucleophilicity of methyl sulfate anion toward *trans*- β -IEPOX was determined to be approximately 0.1. Therefore, tertiary substituted epoxides may provide particularly poor targets for organosulfate nucleophiles even though the neighboring hydroxyl groups of *trans*- β -IEPOX might have been expected to increase the nucleophilicity of such species.

Acid-Catalyzed Epoxide Ring Opening Kinetics. The second-order acid-catalyzed rate constants are listed in Table 4. The rate constants of several of these epoxides were previously measured at 0 degrees C in $\text{HClO}_4/\text{H}_2\text{O}$ solutions and are generally consistent (i.e., 2–3 times smaller)⁴¹ with those determined at room temperature in the present study. It is possible that the use of deuterated solutions in the present study could lead to the observation of different rates of

reaction than would be observed for a normal isotope. However, it is not straightforward to ascertain whether this effect would lead to slower or faster rates of reaction for the deuterated solutions used in the present study.

Rate Constant–Sulfate Nucleophilicity Correlation.

From the results shown in Table 4, it was noted that there appeared to be an inverse correlation between the total sulfate nucleophilicity and the acid-catalyzed epoxide ring opening rate constant for each epoxide species. An approximate linear relationship was obtained by plotting the total sulfate nucleophilicity versus the logarithm of the rate constant, as shown in Figure 3. Since the logarithm of the rate constant is

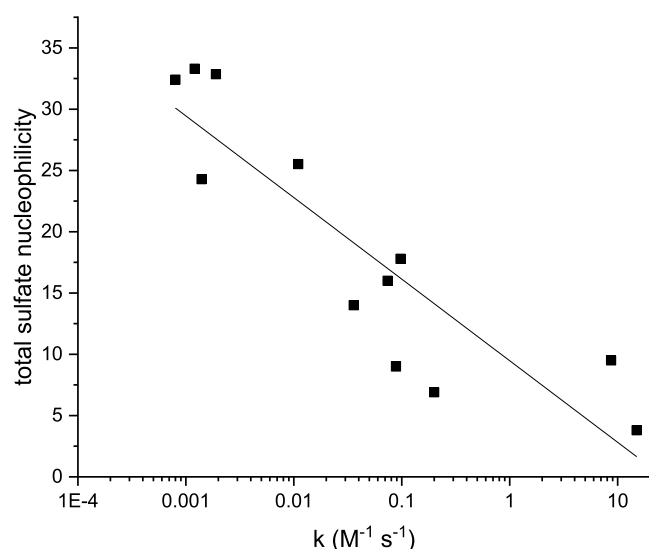


Figure 3. Total sulfate nucleophilicity/acid-catalyzed second-order ring opening epoxide reaction rate constant correlation.

inversely proportional to the activation energy, this finding indicates that nucleophilicity is enhanced for epoxides with higher energy transition states, which is likely related to the qualitative electronic trends noted for the nucleophilic strengths of sulfate and the methyl sulfate anion in their reactions with propylene oxide and its derivatives. In particular, a neighboring electronegative substituent will destabilize the

positively charged transition state by withdrawing electron density—this serves to both increase the energy of the transition state and thereby decrease the ring opening rate constant and increase the effective nucleophilicity of the attacking nucleophile by making the attack site more electropositive.

Atmospheric Implications. In order to assess the relative reactivity of sulfate and bisulfate for different SOA pH conditions, SOA was modeled as fixed 1.0 M total sulfate solutions by carrying out E-AIM calculations with differing amounts of H^+ and NH_4^+ (ranging from 1.0 M H_2SO_4 to 1.0 M $(\text{NH}_4)_2\text{SO}_4$) to provide a charge balance. Figure 4 shows the dependence of the formal molalities of sulfate and bisulfate as a function of pH ($= -\log_{10}(m_{\text{H}^+})$) (panel A) as well as the dependence of the activities of sulfate and bisulfate as a function of $-\log_{10}(a_{\text{H}^+})$ (Panel B). Panel A illustrates the dependence with parameters that do not take into account solution nonideality, while Panel B explicitly uses parameters that reflect the nonideality of the solutions.

These graphs both indicate that sulfate is expected to be the major inorganic sulfur species except for situations of very low acidity ($\text{pH} < 1$). Most estimates of SOA acidity indicate that the average pH values are usually in excess of $\text{pH} = 1$, thus indicating that sulfate is usually the dominant species, although pH values of less than zero are occasionally observed.^{42–44} At the highest acidity level modeled above ($\text{pH} = -0.096$, $-\log_{10}(a_{\text{H}^+}) = 0.01$), the bisulfate activity is calculated to be about 90 times greater than that of sulfate. However, the present study indicates that the molal activity-based nucleophilicity of bisulfate is about 100 times less than that of sulfate. Therefore, even for this extreme acidity case, sulfate is expected to compete with bisulfate as a nucleophilic reaction partner with epoxides due to the nearly offsetting differences in activity (90x greater for bisulfate) and nucleophilic strength (100x greater for sulfate). In summary, under most SOA acidity conditions, sulfate is expected to be the main nucleophilic reaction partner for epoxide reactions, and as shown in Figure 1, these reactions have the capacity to deplete the acidity of the SOA particles on which they occur.

The mole fraction-based nucleophilic strengths of sulfate on the order of 10 (defined relative to water) can be compared to previous nucleophilic strength measurements on the order of

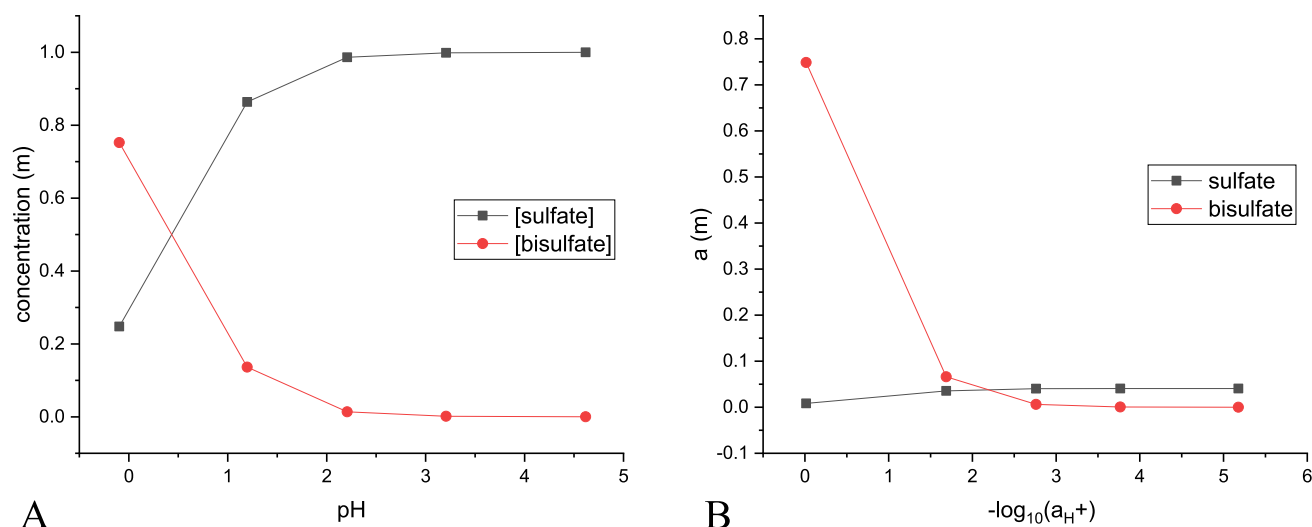


Figure 4. (Panel A) concentration vs pH and (Panel B) activity vs $-\log_{10}(a_{\text{H}^+})$ for model SOA solutions described in text.

unity for alcohols,²⁶ 10 for nitrate,^{12,39} 100 for halides,³⁹ and 1000 for amines.⁴⁵ Therefore, in an aerosol environment in which many different nucleophiles are present, sulfate may be in a competitive situation with other nonwater nucleophiles with respect to the epoxide reaction.

The present results also show that organosulfates are likely to be weak nucleophiles compared to an inorganic sulfate and comparably nucleophilic to bisulfate and water. Indeed, when *trans*- β -IEPOX was directly reacted with a 5.0 M solution of the model organosulfate methyl sulfate anion, only the hydrolysis reaction was observed. It is possible that the methyl sulfate anion is a poor proxy for the various organosulfates that are known to exist on the SOA. However, both the computational basicities and experimental nucleophilicities for methyl sulfate and bisulfate anions were found to be virtually identical in this work, suggesting that the nature of the alkyl group may not have large electronic effects on the nucleophilicity. Previous studies of the effect of neighboring OH moieties on the nucleophilic strength of alcohols showed fairly small electronic effects, but sterically hindered positions were found to significantly reduce nucleophilicity.²⁶ Therefore, the major organosulfate generated from the nucleophilic attack of the sulfate anion on *trans*- β -IEPOX, due to the sterically hindered tertiary position of its OSO_3^- moiety, would be expected to be an even poorer nucleophile than the methyl sulfate anion. However, it is clear from recent HILIC/ESI-MS-based experiments that sulfated dimer species with the same chemical formula as the one shown in Figure 1 (but not necessarily the same structure) have been detected in both laboratory experiments and field environments.²² In the case of laboratory studies of *trans*- β -IEPOX, dimers were measured to be formed on the order of 1% of the amount of the monomers formed from the reaction of *trans*- β -IEPOX with the sulfate anion. Since the upper limit for the relative nucleophilicity of methyl sulfate to sulfate anions in reaction with *trans*- β -IEPOX was found to be about 1%, these results are broadly consistent (with the caveat that the relative concentrations would be needed to make a proper quantitative comparison) with the present work. However, in the aerosol volatility studies in which the individual molecular components of the isoprene-derived SOA were largely not determined, the oligomeric composition was inferred to be much higher.^{19–21} Therefore, it seems unlikely that aqueous phase nucleophilic reactions via the OSO_3^- moiety of organosulfates with atmospherically relevant epoxides such as IEPOX can produce the proportion of oligomers needed to rationalize the previous aerosol volatility studies. A similar conclusion was recently drawn concerning the oligomer-forming potential of the nucleophilic reactions of 2-methyltetrols with IEPOX due to the weak nucleophilicities of polyols such as the 2-methyltetrols.²⁶ Of course, the oligomers observed in other studies may form via pathways other than nucleophilic addition to *trans*- β -IEPOX via OSO_3^- or OH moieties. It is also possible that the phase separation phenomenon^{16,18,46} recently reported for the isoprene-derived SOA may provide reaction environments (such as nonequilibrated nucleophile concentrations or nonaqueous effective solvent situations) that are not well represented by the aqueous media used in the present study.

■ ASSOCIATED CONTENT

Supporting Information

The Supporting Information is available free of charge at <https://pubs.acs.org/doi/10.1021/acsearthspacechem.0c00178>.

NMR assignments, solution parameters, and observed sulfate product yields (PDF)

■ AUTHOR INFORMATION

Corresponding Author

Matthew J. Elrod – Department of Chemistry and Biochemistry, Oberlin College, Oberlin, Ohio 44074, United States;
orcid.org/0000-0002-1656-8261; Email: mjelrod@oberlin.edu

Authors

Erika Aoki – Department of Chemistry and Biochemistry, Oberlin College, Oberlin, Ohio 44074, United States

Jon N. Sarrimanolis – Department of Chemistry and Biochemistry, Oberlin College, Oberlin, Ohio 44074, United States

Sophie A. Lyon – Department of Chemistry and Biochemistry, Oberlin College, Oberlin, Ohio 44074, United States

Complete contact information is available at:

<https://pubs.acs.org/doi/10.1021/acsearthspacechem.0c00178>

Notes

The authors declare no competing financial interest.

■ ACKNOWLEDGMENTS

We thank Santino Stropoli and Daniel Hill for their assistance in preparing the synthesized chemicals. This material is based on the work supported by the National Science Foundation under Grant Nos. 1427949, 1559319, and 1841019.

■ REFERENCES

- (1) Kanakidou, M.; Seinfeld, J. H.; Pandis, S. N.; Barnes, I.; Dentener, F. J.; Facchini, M. C.; Van Dingenen, R.; Ervens, B.; Nenes, A.; Nielsen, C. J.; Swietlicki, E.; Putaud, J. P.; Balkanski, Y.; Fuzzi, S.; Horth, J.; Moortgat, G. K.; Winterhalter, R.; Myhre, C. E. L.; Tsigaridis, K.; Vignati, E.; Stephanou, E. G.; Wilson, J. Organic Aerosol and Global Climate Modelling: A Review. *Atmos. Chem. Phys.* **2005**, *5*, 1053–1123.
- (2) Pope, C. A., III; Dockery, D. W. Health Effects of Fine Particulate Air Pollution: Lines That Connect. *J. Air Waste Manage. Assoc.* **2006**, *56*, 709–742.
- (3) West, J. J.; Cohen, A.; Dentener, F.; Brunekreef, B.; Zhu, T.; Armstrong, B.; Bell, M. L.; Brauer, M.; Carmichael, G.; Costa, D. L.; Dockery, D. W.; Kleeman, M.; Krzyzanowski, M.; Kunzli, N.; Liousse, C.; Lung, S. C.; Martin, R. V.; Poschl, U.; Pope, C. A.; Roberts, J. M.; Russell, A. G.; Wiedinmyer, C. What We Breathe Impacts Our Health: Improving Understanding of the Link between Air Pollution and Health. *Environ. Sci. Technol.* **2016**, *50*, 4895–4904.
- (4) Seinfeld, J. H.; Pandis, S. N., *Atmospheric Chemistry and Physics*. 3rd ed.; John Wiley and Sons, Inc.: New Jersey, 2016.
- (5) Hallquist, M.; Wenger, J. C.; Baltensperger, U.; Rudich, Y.; Simpson, D.; Claeys, M.; Dommen, J.; Donahue, N. M.; George, C.; Goldstein, A. H.; Hamilton, J. F.; Herrmann, H.; Hoffmann, T.; Iinuma, Y.; Jang, M.; Jenkin, M. E.; Jimenez, J. L.; Kiendler-Scharr, A.; Maenhaut, W.; McFiggans, G.; Mentel, T. F.; Monod, A.; Prevot, A. S. H.; Seinfeld, J. H.; Surratt, J. D.; Szmigielski, R.; Wildt, J. The Formation, Properties and Impact of Secondary Organic Aerosol: Current and Emerging Issues. *Atmos. Chem. Phys.* **2009**, *9*, 5155–5236.

- (6) Chen, Q.; Farmer, D. K.; Rizzo, L. V.; Pauliquevis, T.; Kuwata, M.; Karl, T. G.; Guenther, A.; Allan, J. D.; Coe, H.; Andreae, M. O.; Pöschl, U.; Jimenez, J. L.; Artaxo, P.; Martin, S. T. Submicron Particle Mass Concentrations and Sources in the Amazonian Wet Season (Amaze-08). *Atmos. Chem. Phys.* **2015**, *15*, 3687–3701.
- (7) McNeill, V. F. Aqueous Organic Chemistry in the Atmosphere: Sources and Chemical Processing of Organic Aerosols. *Environ. Sci. Technol.* **2015**, *49*, 1237–1244.
- (8) Paulot, F.; Crounse, J. D.; Kjaergaard, H. G.; Kurten, A.; St. Clair, J. M.; Seinfeld, J. H.; Wennberg, P. O. Unexpected Epoxide Formation in the Gas-Phase Photooxidation of Isoprene. *Science* **2009**, *325*, 730–733.
- (9) Cole-Filiipiak, N. C.; O'Connor, A. E.; Elrod, M. J. Kinetics of the Hydrolysis of Atmospherically Relevant Isoprene-Derived Hydroxy Epoxides. *Environ. Sci. Technol.* **2010**, *44*, 6718–6723.
- (10) Surratt, J. D.; Chan, A. W. H.; Eddingsaas, N. C.; Chan, M.; Loza, C. L.; Kwan, A. J.; Hersey, S. P.; Flagan, R. C.; Wennberg, P. O.; Seinfeld, J. H. Reactive Intermediates Revealed in Secondary Organic Aerosol Formation from Isoprene. *Proc. Natl. Acad. Sci.* **2010**, *107*, 6640–6645.
- (11) Lin, Y.-H.; Zhang, Z.; Docherty, K. S.; Zhang, H.; Budisulistiorini, S. H.; Rubitschun, C. L.; Shaw, S. L.; Knipping, E. M.; Edgerton, E. S.; Kleindienst, T. E.; Gold, A.; Surratt, J. D. Isoprene Epoxydiols as Precursors to Secondary Organic Aerosol Formation: Acid-Catalyzed Reactive Uptake Studies with Authentic Compounds. *Environ. Sci. Technol.* **2012**, *46*, 250–258.
- (12) Darer, A. I.; Cole-Filiipiak, N. C.; O'Connor, A. E.; Elrod, M. J. Formation and Stability of Atmospherically Relevant Isoprene-Derived Organosulfates and Organonitrates. *Environ. Sci. Technol.* **2011**, *45*, 1895–1902.
- (13) Claeys, M.; Graham, B.; Vas, G.; Wang, W.; Vermeylen, R.; Pashynska, V.; Jan, C.; Guyon, P.; Andreae, M. O.; Artaxo, P.; Maenhaut, W. Formation of Secondary Organic Aerosols through Photooxidation of Isoprene. *Science* **2004**, *303*, 1173–1176.
- (14) Surratt, J. D.; Kroll, J. H.; Kleindienst, T. E.; Edney, E. O.; Claeys, M.; Sorooshian, A.; Ng, N. L.; Offenberg, J. H.; Lewandowski, M.; Jaoui, M.; Flagan, R. C.; Seinfeld, J. H. Evidence for Organosulfates in Secondary Organic Aerosol. *Environ. Sci. Technol.* **2007**, *41*, S17–S27.
- (15) Nguyen, T. B.; Coggon, M. M.; Bates, K. H.; Zhang, X.; Schwantes, R. H.; Schilling, K. A.; Loza, C. L.; Flagan, R. C.; Wennberg, P. O.; Seinfeld, J. H. Organic Aerosol Formation from the Reactive Uptake of Isoprene Epoxydiols (IEPOX) onto Non-Acidified Inorganic Seeds. *Atmos. Chem. Phys.* **2014**, *14*, 3497–3510.
- (16) Zhang, Y.; Chen, Y.; Lei, Z.; Olson, N. E.; Riva, M.; Koss, A. R.; Zhang, Z.; Gold, A.; Jayne, J. T.; Worsnop, D. R.; Onasch, T. B.; Kroll, J. H.; Turpin, B. J.; Ault, A. P.; Surratt, J. D. Joint Impacts of Acidity and Viscosity on the Formation of Secondary Organic Aerosol from Isoprene Epoxydiols (IEPOX) in Phase Separated Particles. *ACS Earth Space Chem.* **2019**, *3*, 2646–2658.
- (17) Hettiyadura, A. P. S.; Xu, L.; Jayarathne, T.; Skog, K.; Guo, H.; Weber, R. J.; Nenes, A.; Keutsch, F. N.; Ng, N. L.; Stone, E. A. Source Apportionment of Organic Carbon in Centreville, AL Using Organosulfates in Organic Tracer-Based Positive Matrix Factorization. *Atmos. Environ.* **2018**, *186*, 74–88.
- (18) Riva, M.; Chen, Y.; Zhang, Y.; Lei, Z.; Olson, N. E.; Boyer, H. C.; Narayan, S.; Yee, L. D.; Green, H. S.; Cui, T.; Zhang, Z.; Baumann, K.; Fort, M.; Edgerton, E.; Budisulistiorini, S. H.; Rose, C. A.; Ribeiro, I. O.; RL, E. O.; Dos Santos, E. O.; Machado, C. M. D.; Szopa, S.; Zhao, Y.; Alves, E. G.; de Sa, S. S.; Hu, W.; Knipping, E. M.; Shaw, S. L.; Duvoisin Junior, S.; de Souza, R. A. F.; Palm, B. B.; Jimenez, J. L.; Glasius, M.; Goldstein, A. H.; Pye, H. O. T.; Gold, A.; Turpin, B. J.; Vizuete, W.; Martin, S. T.; Thornton, J. A.; Dutcher, C. S.; Ault, A. P.; Surratt, J. D. Increasing Isoprene Epoxydiol-to-Inorganic Sulfate Aerosol Ratio Results in Extensive Conversion of Inorganic Sulfate to Organosulfur Forms: Implications for Aerosol Physicochemical Properties. *Environ. Sci. Technol.* **2019**, *53*, 8682–8694.
- (19) Lopez-Hilfiker, F. D.; Mohr, C.; D'Ambro, E. L.; Lutz, A.; Riedel, T. P.; Gaston, C. J.; Iyer, S.; Zhang, Z.; Gold, A.; Surratt, J. D.; Lee, B. H.; Kurten, T.; Hu, W. W.; Jimenez, J.; Hallquist, M.; Thornton, J. A. Molecular Composition and Volatility of Organic Aerosol in the Southeastern U.S.: Implications for IEPOX Derived SOA. *Environ. Sci. Technol.* **2016**, *50*, 2200–2209.
- (20) Hu, W.; Palm, B. B.; Day, D. A.; Campuzano-Jost, P.; Krechmer, J. E.; Peng, Z.; de Sá, S. S.; Martin, S. T.; Alexander, M. L.; Baumann, K.; Hacker, L.; Kiendler-Scharr, A.; Koss, A. R.; de Gouw, J. A.; Goldstein, A. H.; Seco, R.; Sjostedt, S. J.; Park, J.-H.; Guenther, A. B.; Kim, S.; Canonaco, F.; Prévôt, A. S. H.; Brune, W. H.; Jimenez, J. L. Volatility and Lifetime against OH Heterogeneous Reaction of Ambient Isoprene-Epoxydiols-Derived Secondary Organic Aerosol (IEPOX-SOA). *Atmos. Chem. Phys.* **2016**, *16*, 11563–11580.
- (21) D'Ambro, E. L.; Lee, B. H.; Liu, J.; Shilling, J. E.; Gaston, C. J.; Lopez-Hilfiker, F. D.; Schobesberger, S.; Zaveri, R. A.; Mohr, C.; Lutz, A.; Zhang, Z.; Gold, A.; Surratt, J. D.; Rivera-Rios, J. C.; Keutsch, F. N.; Thornton, J. A. Molecular Composition and Volatility of Isoprene Photochemical oxidation secondary organic Aerosol under low- and high-NO_x conditions. *Atmos. Chem. Phys.* **2017**, *17*, 159–174.
- (22) Cui, T.; Zeng, Z.; dos Santos, E. O.; Zhang, Z.; Chen, Y.; Zhang, Y.; Rose, C. A.; Budisulistiorini, S. H.; Collins, L. B.; Bodnar, W. M.; de Souza, R. A. F.; Martin, S. T.; Machado, C. M. D.; Turpin, B. J.; Gold, A.; Ault, A. P.; Surratt, J. D. Development of a Hydrophilic Interaction Liquid Chromatography (HILIC) Method for the Chemical Characterization of Water-Soluble Isoprene Epoxydiol (IEPOX)-Derived Secondary Organic Aerosol. *Environ. Sci.: Processes Impacts* **2018**, *20*, 1524–1536.
- (23) Glasius, M.; Goldstein, A. H. Recent Discoveries and Future Challenges in Atmospheric Organic Chemistry. *Environ. Sci. Technol.* **2016**, *50*, 2754–2764.
- (24) Budisulistiorini, S. H.; Nenes, A.; Carlton, A. G.; Surratt, J. D.; McNeill, V. F.; Pye, H. O. T. Simulating Aqueous-Phase Isoprene-Epoxydiol (IEPOX) Secondary Organic Aerosol Production During the 2013 Southern Oxidant and Aerosol Study SOAS. *Environ. Sci. Technol.* **2017**, *51*, 5026–5034.
- (25) Pye, H. O. T.; Pinder, R. W.; Piletic, I. R.; Xie, Y.; Capps, S. L.; Lin, Y.-H.; Surratt, J. D.; Zhang, Z.; Gold, A.; Lueken, D. J.; Hutzell, W. T.; Jaoui, M.; Offenberg, J. H.; Kleindienst, T. E.; Lewandowski, M.; Edney, E. O. Epoxide Pathways Improve Model Predictions of Isoprene Markers and Reveal Key Role of Acidity in Aerosol Formation. *Environ. Sci. Technol.* **2013**, *47*, 11056–11064.
- (26) Stropoli, S. J.; Miner, C. R.; Hill, D. R.; Elrod, M. J. Assessing Potential Oligomerization Reaction Mechanisms of Isoprene Epoxydiols on Secondary Organic Aerosol. *Environ. Sci. Technol.* **2019**, *53*, 176–184.
- (27) Clegg, S. L.; Brimblecombe, P.; Exler, A. S. A Thermodynamic Model of the System H⁺-NH₄⁺-SO₄²⁻-NO₃⁻-H₂O at Tropospheric Temperatures. *J. Phys. Chem. A* **1998**, *102*, 2137–2154.
- (28) Watanabe, A. C.; Stropoli, S. J.; Elrod, M. J. Assessing the Potential Mechanisms of Isomerization Reactions of Isoprene Epoxydiols on Secondary Organic Aerosol. *Environ. Sci. Technol.* **2018**, *52*, 8346–8354.
- (29) Jacobs, M. I.; Darer, A. I.; Elrod, M. J. Rate Constants and Products of the OH Reaction with Isoprene-Derived Epoxides. *Environ. Sci. Technol.* **2013**, *47*, 12868–12876.
- (30) Froese, R. D. J.; Humbel, S.; Svensson, M.; Morokuma, K. IMOMO(G2MS): A New High-Level G2-Like Method for Large Molecules and Its Applications to Diels–Alder Reactions. *J. Phys. Chem. A* **1997**, *101*, 227–233.
- (31) Curtiss, L. A.; Raghavachari, K.; Redfern, P. C.; Pople, J. A. Assessment of Gaussian-2 and Density Functional Theories for the Computation of Enthalpies of Formation. *J. Chem. Phys.* **1997**, *106*, 1063–1079.
- (32) Tomasi, J.; Mennucci, B.; Cammi, R. Quantum Mechanical Continuum Solvation Models. *Chem. Rev.* **2005**, *105*, 2999–3094.
- (33) Frisch, M. J. T.; Schlegel, H. B.; Scuseria, G. E.; Robb, M. A.; Cheeseman, J. R.; Montgomery, Jr., J. A.; Vreven, T.; Kudin, K. N.; Burant, J. C.; Millam, J. M.; Iyengar, S. S.; Tomasi, J.; Barone, V.;

Mennucci, B.; Cossi, M.; Scalmani, G.; Rega, N.; Petersson, G. A.; Nakatsuji, H.; Hada, M.; Ehara, M.; Toyota, K.; Fukuda, R.; Hasegawa, J.; Ishida, M.; Nakajima, T.; Honda, Y.; Kitao, O.; Nakai, H.; Klene, M.; Li, X.; Knox, J. E.; Hratchian, H. P.; Cross, J. B.; Bakken, V.; Adamo, C.; Jaramillo, J.; Gomperts, R.; Stratmann, R. E.; Yazyev, O.; Austin, A. J.; Cammi, R.; Pomelli, C.; Ochterski, J. W.; Ayala, P. Y.; Morokuma, K.; Voth, G. A.; Salvador, P.; Dannenberg, J. J.; Zakrzewski, V. G.; Dapprich, S.; Daniels, A. D.; Strain, M. C.; Farkas, O.; Malick, D. K.; Rabuck, A. D.; Raghavachari, K.; Foresman, J. B.; Ortiz, J. V.; Cui, Q.; Baboul, A. G.; Clifford, S.; Cioslowski, J.; Stefanov, B. B.; Liu, G.; Liashenko, A.; Piskorz, P.; Komaromi, I.; Martin, R. L.; Fox, D. J.; Keith, T.; Al-Laham, M. A.; Peng, C. Y.; Nanayakkara, A.; Challacombe, M.; Gill, P. M. W.; Johnson, B.; Chen, W.; Wong, M. W.; Gonzalez, C.; Pople, J. A., *Gaussian 03*. Gaussian, Inc.: Wallingford, CT, 2003.

(34) Cappa, C. D.; Elrod, M. J. A Computational Investigation of the Electron Affinity of CO_3^- and the Thermodynamic Feasibility of $\text{CO}_3^-(\text{H}_2\text{O})_N + \text{Rooh}$ Reactions. *Phys. Chem. Chem. Phys.* **2001**, *3*, 2986–2994.

(35) Whalen, D. L. Mechanisms of Hydrolysis and Rearrangements of Epoxides. *Adv. Phys. Org. Chem.* **2005**, *59*, 247–799.

(36) Carey, F., Robert, G. *Organic Chemistry*. New York, 2013.

(37) Minerath, E. C.; Elrod, M. J. Assessing the Potential for Diol and Hydroxy Sulfate Ester Formation from the Reaction of Epoxides in Tropospheric Aerosols. *Environ. Sci. Technol.* **2009**, *43*, 1386–1392.

(38) Eddingsaas, N. C.; VanderVelde, D. G.; Wennberg, P. O. Kinetics and Products of the Acid-Catalyzed Ring-Opening of Atmospherically Relevant Butyl Epoxy Alcohols. *J. Phys. Chem. A* **2010**, *114*, 8106–8113.

(39) Minerath, E. C.; Schultz, M. P.; Elrod, M. J. Kinetics of the Reactions of Isoprene-Derived Epoxides in Model Tropospheric Aerosol Solutions. *Environ. Sci. Technol.* **2009**, *43*, 8133–8139.

(40) Bates, K. H.; Crounse, J. D.; St. Clair, J. M.; Bennett, N. B.; Nguyen, T. B.; Seinfeld, J. H.; Stoltz, B. M.; Wennberg, P. O. Gas Phase Production and Loss of Isoprene Epoxydiols. *J. Phys. Chem. A* **2014**, *118*, 1237–1246.

(41) Pritchard, J. G.; Long, F. A. Kinetics and Mechanism of the Acid-Catalyzed Hydrolysis of Substituted Ethylene Oxides. *J. Am. Chem. Soc.* **1956**, *78*, 2667–2670.

(42) Pye, H. O. T.; Nenes, A.; Alexander, B.; Ault, A. P.; Barth, M. C.; Clegg, S. L.; Collett, J. L., Jr.; Fahey, K. M.; Hennigan, C. J.; Herrmann, H.; Kanakidou, M.; Kelly, J. T.; Ku, I. T.; McNeill, V. F.; Riemer, N.; Schaefer, T.; Shi, G.; Tilgner, A.; Walker, J. T.; Wang, T.; Weber, R.; Xing, J.; Zaveri, R. A.; Zuend, A. The Acidity of Atmospheric Particles and Clouds. *Atmos. Chem. Phys.* **2020**, *20*, 4809–4888.

(43) Shi, G.; Xu, J.; Peng, X.; Xiao, Z.; Chen, K.; Tian, Y.; Guan, X.; Feng, Y.; Yu, H.; Nenes, A.; Russell, A. G. Ph of Aerosols in a Polluted Atmosphere: Source Contributions to Highly Acidic Aerosol. *Environ. Sci. Technol.* **2017**, *51*, 4289–4296.

(44) Craig, R. L.; Nandy, L.; Axson, J. L.; Dutcher, C. S.; Ault, A. P. Spectroscopic Determination of Aerosol Ph from Acid-Base Equilibria in Inorganic, Organic, and Mixed Systems. *J. Phys. Chem. A* **2017**, *121*, 5690–5699.

(45) Stropoli, S. J.; Elrod, M. J. Assessing the Potential for the Reactions of Epoxides with Amines on Secondary Organic Aerosol Particles. *J. Phys. Chem. A* **2015**, *119*, 10181–10189.

(46) Olson, N. E.; Lei, Z.; Craig, R. L.; Zhang, Y.; Chen, Y.; Lambe, A. T.; Zhang, Z.; Gold, A.; Surratt, J. D.; Ault, A. P. Reactive Uptake of Isoprene Epoxydiols Increases the Viscosity of the Core of Phase-Separated Aerosol Particles. *ACS Earth Space Chem.* **2019**, *3*, 1402–1414.